

Million-Atom Pseudopotential Calculation of Γ - X Mixing in GaAs_yAlAs Superlattices and Quantum Dots

Lin-Wang Wang, Alberto Franceschetti, and Alex Zunger
 National Renewable Energy Laboratory, Golden, Colorado 80401
 (Received 1 November 1996)

We have developed a “linear combination of bulk bands” method that permits atomistic, pseudopotential electronic structure calculations for 10^6 atom nanostructures. Application to sGaAs_{*m*}yAlAs_{*n*} (001) superlattices (SL’s) reveals even-odd oscillations in the G- X coupling magnitude V_{GX} , which vanishes for n - odd, even for *abrupt* and *segregated* SL’s, respectively. Surprisingly, in contrast with recent expectations, 0D quantum dots are found here to have a *smaller* G- X coupling than equivalent 2D SL’s. Our analysis shows that for large quantum dots this is largely due to the existence of level repulsion from *many* X states. [S0031-9007(97)02839-1]

PACS numbers: 73.20.Dx, 71.15.Hx, 73.61.Ey

The crossover from direct band gap to indirect band gap (e.g., $G \rightarrow X$) as a function of an external parameter is common in semiconductor physics. It is seen in (i) zinc blende materials (GaAs [1], InP [2]) as a function of pressure, (ii) alloys (Al_{*x*}Ga_{*1-2x*}As [3], Ga_{*x*}In_{*1-2x*}P [4]) as a function of composition x , and (iii) in superlattices (SL’s) [5–9] and quantum dots [10,11] as a function of size or external pressure. While in cases (i) and (ii) the transition is believed to be first order [3], in nanostructures [case (iii)] the lack of translational invariances causes a quantum-mechanical mixing between the zone center G and the zone edge X states [12], measured by the coupling matrix element V_{GX} . Although small in magnitude ($V_{GX} \sim 10$ meV), the G- X coupling has profound consequences on the properties of the system, leading, for example, to the appearance of indirect transitions without phonon intervention [7,8], to characteristic pressure-induced changes of the photoluminescence intensity [9,10], to resonant tunneling in electronic transmission between GaAs quantum wells separated by an AlAs barrier [13] and to level splitting (“avoided crossing”) in the pressure, electric-field, and magnetic-field induced G- X transition [5,6].

The significance of this small but crucial quantum-mechanical coupling has prompted attempts to measure V_{GX} in sGaAs_{*m*}yAlAs_{*n*} (001) superlattices, producing, however, widely scattered results: Meynadier *et al.* [5] found from the electric-field dependence of the photoluminescence energy $V_{GX} \sim 12.28$ meV, while Pulsford *et al.* [6] found from the magnetic-field induced gap in the Landau level $V_{GX} \sim 9.3$ meV. Measurements of the valence (y) to conduction (c) $G_y \leftrightarrow G_c$ and $G_y \leftrightarrow X_c$ emission [7] or absorption [8] fitted to theoretical models produced $V_{GX} \sim 10.10$ meV in Ref. [7] and $V_{GX} \sim 4.10$ meV in Ref. [8].

The calculation of V_{GX} is difficult, as highlighted by the fact that the central approximation underlying the “standard model” of nanostructure physics—the conventional $\mathbf{k} \cdot \mathbf{p}$ model [14]—leads to $V_{GX} = 0$. Tight-binding

($\mathbf{k} = \mathbf{0}$) bulk Bloch functions $u_{n,0}$ are used to construct the basis functions $f_{a,\mathbf{r}} = u_{n,0} e^{i\mathbf{k}\cdot\mathbf{r}}$. The wave function of the nanostructure is then expanded as

$$c_{i,\mathbf{r}} = \sum_{n,\mathbf{k}} C_{n,\mathbf{k}}^{s,jl} f_{u_{n,0},\mathbf{r}} e^{i\mathbf{k}\cdot\mathbf{r}}. \quad (2)$$

The disadvantage of this approach is that it is unable to reproduce the band structure across the Brillouin zone; in particular, the bulk X_{1c} state is misplaced by ~ 10 eV, as recently shown by Wood *et al.* [23,24], with the consequence that $V_{GX} = 0$ for all nanostructures.

The solution to this dilemma is to replace the zone-center states $u_{n,0}$ in Eq. (2) with the bulk Bloch states $u_{n,\mathbf{k}}$, leading to the linear combination of bulk bands method. For a periodic system consisting of materials A and B , Eq. (2) becomes

$$c_{i,\mathbf{r}} = \sum_{s=A,B} \sum_{n,\mathbf{k}} C_{n,\mathbf{k},\sigma}^{s,jl} f_{u_{n,\mathbf{k}}^s,\mathbf{r}} e^{i\mathbf{k}\cdot\mathbf{r}}, \quad (3)$$

where the first sum runs over the constituent materials A and B , and the second sum runs over the bulk band index n and the supercell reciprocal lattice vectors \mathbf{k} belonging to the first Brillouin zone of the underlying lattice. The advantage of the LCBB method over the conventional $\mathbf{k} \cdot \mathbf{p}$ method is that off-G states $u_{n,\mathbf{k}}^s$ of both materials can be directly included in the basis set, thus eliminating the need for hundreds of \mathbf{k} -

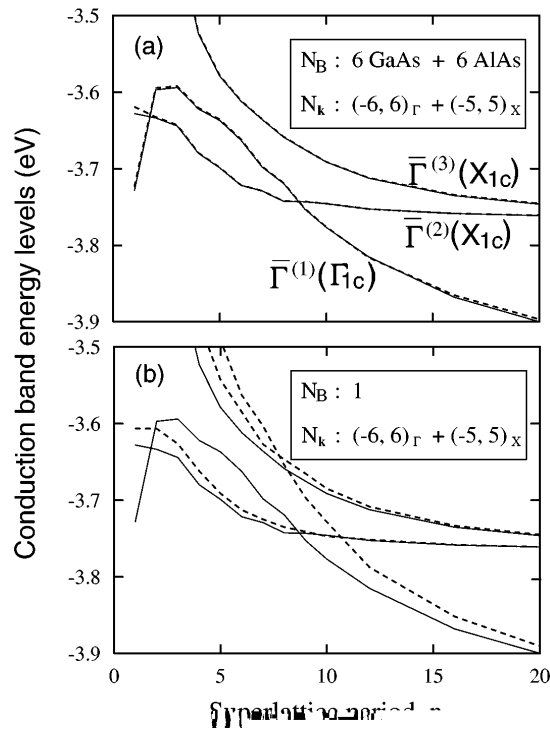


FIG. 1. Energy of the three lowest conduction states at the Γ point of (001) $s\text{GaAs}_n\text{yAlAs}_d_n$ superlattices, obtained using different truncations (insets) in the number of bands N_B and the number of \mathbf{k} points $N_{\mathbf{k}}$ in Eq. (3).

distance between the G and X curves, is 0.9 meV for $n = 20$. This value should be compared with 1.2 meV we obtained from an exact calculation (i.e., no truncation in N_B or $N_{\mathbf{k}}$). Figure 2(c) shows the VBM \rightarrow CBM (conduction-band minimum) momentum transition matrix element $|\langle \mathbf{k}_{\text{CBM}} | \mathbf{p} | \mathbf{k}_{\text{VBM}} \rangle|^2$ as a function of pressure. We see that unlike alloys [3], the transition in superlattices (and dots) is *not* first order. The finite G-X coupling V_{GX} leads to the presence of some G character even in the “indirect gap region” ($P \ S \ P_c$), producing there a *finite optical transition probability*.

In the above calculations we assumed ideal, sharp interfaces. To see whether interfacial roughness, present in real samples, can quench the G-X coupling, we have compared V_{GX} for $s\text{GaAs}_n\text{yAlAs}_d_n$ superlattices with sharp interfaces and with realistic segregated profiles obtained by solving the segregation equation [27]. The results (Fig. 3) show that while segregation reduces V_{GX} by about a factor of 2, the odd-even oscillations of V_{GX} with the period n are not washed out. In fact, while for *abrupt* SL's [Fig. 3(a)], $V_{GX} = 0$ for $n = \text{odd}$, in segregated SL's, $V_{GX} \neq 0$ for $n = \text{even}$ [Fig. 3(b)]. Our calculated $V_{GX} = 1.24$ meV for a sharp $s\text{GaAs}_{12}\text{yAlAs}_{28}$ SL, is in excellent agreement with the experimental [5] value of 1.25 meV.

We next study G-X coupling in GaAs dots embedded in AlAs matrix. To compare meaningfully the G-X coupling in quantum dots and superlattices, we have chosen a particular dot geometry (inset of Fig. 4): 20 monolayers

(ML) of GaAs sandwiched by 20 ML of AlAs in the [001] direction and N ML of GaAs surrounded by 20 ML of AlAs in the [110] and $\bar{1}\bar{1}0g$ directions. Thus, when $N \rightarrow \infty$ the quantum dot merges into a 20×20 [001] superlattice. The pressure dependence of the transition energies and of the momentum matrix element for a $N = 140$ quantum dot are shown in Figs. 2(b) and 2(c) (where the supercell contains 2×10^6 atoms). The calculation takes ~ 30 min on a IBM RSY6000 work station model 590 for one pressure value. We find that the G-X coupling in these QD's is *smaller* than in the corresponding 20×20 superlattice [compare Fig. 2(a)]. Furthermore, as shown in Fig. 4, the anticrossing gap $\Delta E_{\text{min}} = 2V_{GX}$ in two level systems) in dots does not approach the superlattice value when N increases. There are two reasons for this: (i) For small dots, the 20 ML barrier region of AlAs in [110] and

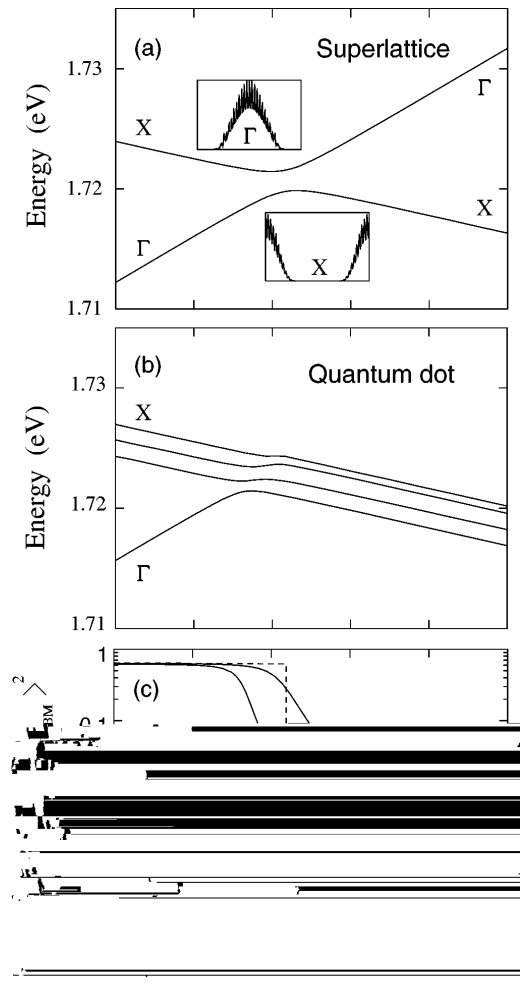


FIG. 2. Pressure dependence of the transition energies from the VBM to the G and X-derived conduction bands (a) and (b) and transition probabilities (c) of a $s\text{GaAs}_{20}\text{yAlAs}_{20}$ superlattice and a $20 \times 140 \times 140$ quantum dot. The insets in part (a) show the G and X wave functions along the [001] direction of the superlattice. The dashed line in part (c) gives the SL transition probability expected in the absence of G-X coupling.

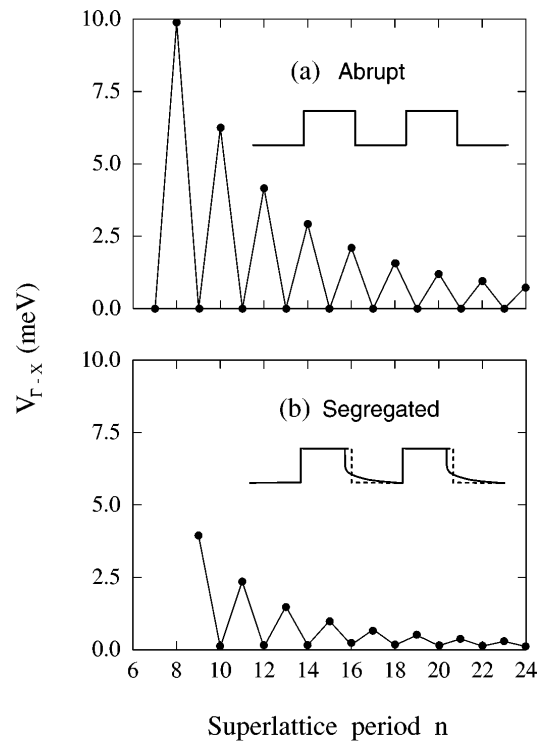


FIG. 3. G-X